Research Article
Curious Case of Bactericidal Action of ZnO

Somnath Ghosh,[1,2] R. Gowri Sankar,[2] and V. Vandana[2]

[1] *Solid State and Structural Chemistry Unit (SSCU), Indian Institute of Science (IISc), Bangalore 560012, India*
[2] *Department of Chemistry, Central Research Laboratory, Gandhi Institute of Technology and Management (GITAM) University, Rushikonda, Visakhapatnam, Andhra Pradesh 530045, India*

Correspondence should be addressed to Somnath Ghosh; ghoshmnth@gmail.com

ZnO nanoparticles (NPs) are well known for their bactericidal properties. Various mechanisms are proposed for their bactericidal activity. An ambiguity still prevails to know which mechanism or property is mainly influencing the bactericidal activity of ZnO NPs. The antibacterial properties of ZnO NPs were investigated against both Gram-positive and Gram-negative bacteria. Different ZnO samples with different degrees of surface oxygen vacancies were prepared from ZnO_2. The surface oxygen vacancy and thereby reactive oxygen species (ROS) production in aqueous ZnO solution are quantified by photoluminescence (PL) and electron paramagnetic resonance (EPR) spin trapping experiments, respectively. Systematic experiments have been performed to validate a precise antibacterial mechanism of ZnO particle.

1. Introduction

The rapid development of nanotechnology emerges in a diverse range of nanomaterials and nanoproducts [1]. Various desired targets have been accomplished in order to employ materials in medicinal fields by maneuvering them at their atomic size scale [2, 3] through nanotechnology. Unfortunately, many such benevolent materials develop toxicity. As toxicities are selective to biological systems, nanomaterials are well exploited for antibacterial applications. To combat bacterial infections metal and metal oxide NPs in various forms are well studied [4–15].

The exposure of such NPs in the environment demands a fundamental understanding about their mode and range of toxicity. Their mode or modes of action towards bacteria remained ambiguous.

ZnO NPs have been extensively used as antibacterial agents for water purification [16–19], biofilm prevention [20–22], sunscreen lotion [23, 24], wound dressing [25], and so forth. Protection against intestinal bacterial infections by bulk ZnO was reported in late 1990s [26, 27] though its bactericidal activity against a broad spectrum of bacteria (e.g., *Staphylococcus aureus*, *Escherichia coli*, *Bacillus subtilis*, *Streptococcus agalactiae*, etc.) was revealed little late when ZnO NPs were exposed to bacterial solution [28–32]. Although the antimicrobial properties of ZnO NPs have been utilized to kill bacteria in different issues, their mechanistic pathways are still imprecise. The mechanisms of antibacterial property of ZnO NPs so far proposed are as follows: (i) physical attack of ZnO NPs on the bacteria [18, 33, 34] (ZnO NPs can adhere to the bacterial cell wall surface and eventually pierce into cell leading to bacterial death by membrane disruption), (ii) oxidative stress generated by particles in solutions [35, 36] (hydroxyl radials are the result of interaction of ZnO NPs with aqueous solution which causes oxidation of bacterial metabolic enzyme leading to bacterial death), and (iii) solubility of NPs in aqueous solution [37, 38]. But none of them is solely responsible on a "one fits all" basis for the desired activity as reported in the literature. The above-mentioned different mechanisms play a role in the bactericidal activity because of size, surface oxygen vacancy, and active surface area of the ZnO particles. A careful investigation is required to evaluate the influence of each such property towards the toxicity of bacteria.

The antibacterial properties of ZnO NPs were investigated against both Gram-positive and Gram-negative bacteria. During bactericidal activity study various properties (e.g., particle size, solubility, surface area, etc.) of ZnO samples

were maintained unaltered when varying the other (e.g., reactive oxygen species (ROS) production, surface defect) through simple chemical route to correlate the antibacterial activity of ZnO with such property. Similarly, when solubility of ZnO samples was varied, ROS production was arrested by glutathione (GSH) in order to eliminate or establish the possibility of oxidative stress mechanism for their bactericidal action. These systematic studies state that bactericidal efficiency of ZnO is little higher for Gram-positive *Staphylococcus aureus* ATCC 25923 compared to Gram-negative *Escherichia coli* MTCC 1302. It has been found that as the surface area increases the solubility of the same sized different ZnO samples in saline water increases and also the bactericidal activity. Interestingly, when ROS production was stopped by employing GSH, bactericidal activity for each of the samples decreases a little. When the amount of ROS production was raised by creating more surface defects in ZnO samples maintaining the same solubility, the bactericidal activity increases with the rise in ROS production. Surprisingly for these samples when ROS production in aqueous solution was blocked bactericidal activity decreases compared to when ROS production was not arrested. But level of antibacterial activity prevails similarly within those samples after ROS production was blocked. The whole understanding of all the observations says that each of these individual physicochemical properties of ZnO samples contributes individually towards the killing of bacteria and noticeably the contribution by ROS production due to surface defect in account of bactericidal activity is the leading part.

2. Experimental Section

2.1. Materials. Zinc acetate dihydrate (S D Fine-Chem Pvt. Ltd., India), diethylene glycol (Merck, India), hydrogen peroxide (30%, S D Fine-Chem Pvt. Ltd., India), $2',7'$-dichlorofluorescein diacetate (DCFH-DA), glutathione (GSH), 5,5-dimethyl-1-pyrroline-N-oxide (DMPO) (Sigma Aldrich Chemical Co. Inc., Germany), and nutrient broth (Hi-Media Laboratories Ltd., India) were used as such without further purification. *Escherichia coli* MTCC 1302 and *Staphylococcus aureus* ATCC 25923 (M.S. Ramaiah Hospital, Bangalore) were used for the bacterial studies.

2.2. Synthesis of ZnO Submicron Particles. Zinc acetate dihydrate (0.9855 gm) was added to 45 mL of diethylene glycol (DEG) with vigorous stirring for 0.5 h at room temperature. The mixture was refluxed at 180°C for 1 h, similar to the procedure described by Ghosh et al. [18]. A milky white precipitate appeared at the end of the reaction indicating the formation of ZnO. The obtained milky precipitate was centrifuged, separated, and washed with ethanol several times by repeated sonication-centrifugation process. The precipitate so obtained was dried under vacuum at 60°C for 6 h and characterized by powder X-ray diffraction.

2.3. Synthesis of ZnO$_2$. The pristine ZnO powder was stirred with 30 mL of aqueous KOH (1 M) solution for 2 h at room temperature and the solution was then washed with water and 50 mL of H_2O_2 (30%) was added, and stirring continued for 24 h at 45°C. The precipitate was washed with water and dried under vacuum and characterized by powder X-ray diffraction, thermogravimetric study.

2.4. Synthesis of Various ZnO Samples from ZnO$_2$. The obtained ZnO$_2$ was heated at 230°C in air and also at 300°C, 400°C, and 500°C under H$_2$ (5% H$_2$ and 95% Ar) atmosphere (flow rate 10 mL/min) for 3 h. Heated samples were designated as ZnO-H, ZnO-300, ZnO-400, and ZnO-500, respectively, and characterized by powder X-ray diffraction.

2.5. DCFH-DA Test. A fluorescence experiment was carried out using a sensitive probe, $2',7'$-dichlorofluorescein diacetate (DCFH-DA), for the detection of ROS by incubating the samples in 30 mL of 0.05×10^{-3} M DCFH-DA solution for 2 h. The colourless DCFH-DA solution changes to green upon exposure with samples and imparts a fluorescence peak at ~525 nm (excited at 485 nm) which indicates the samples produced ROS in aqueous solution.

2.6. Suppression of ROS Production from Aqueous ZnO by GSH Treatment. Glutathione (γ-glutamylcysteinylglycine, GSH), a sulfhydryl (–SH) antioxidant, an antitoxin, is sued for the suppression of ROS as produced from aqueous ZnO solution. Being water soluble and having facile electron donating power, GSH first arrests ROS (i.e., hydroxyl radical, OH$^\bullet$) by reducing them. Various aqueous ZnO samples were incubated with excess GSH till the solution became colorless and hence nonfluorescent (i.e., no peak at ~525 nm when excited at 485 nm).

2.7. Minimum Inhibition Concentration (MIC). The MIC is the lowest concentration at which a material exhibits antimicrobial activity and this was done by serial dilution techniques. Sterile test tubes were taken separately with 9.9 mL of saline water, inoculated with corresponding microorganisms (fresh culture, mid-log phase, OD600 ~0.045–0.050), and diluted up to 10^8 CFU mL^{-1}. Different concentrations (5–200 μg mL^{-1}) of various ZnO samples were added to individual test tubes. After 4 h incubation at 37°C, each 0.1 mL of this solution was taken and plated in sterile nutrient agar plates and the plates were incubated at 37°C overnight and colonies were counted to determine the MIC.

3. Instrumentation and Characterization

3.1. Powder X-Ray Diffraction (XRD). Powder XRD patterns of the prepared ZnO were recorded on Philips XRD "X" PERT PRO diffractometer using Cu-Kα radiation ($\lambda = 1.5438$ Å) as X-ray source.

3.2. Inductively Coupled Plasma-Optical Emission Spectrophotometry (ICPOES). The amount of ZnO dissolved in known volume of saline water for different samples was estimated using Perkin-Elmer optima 2100 ICPOES at $\lambda = 213.8$ nm.
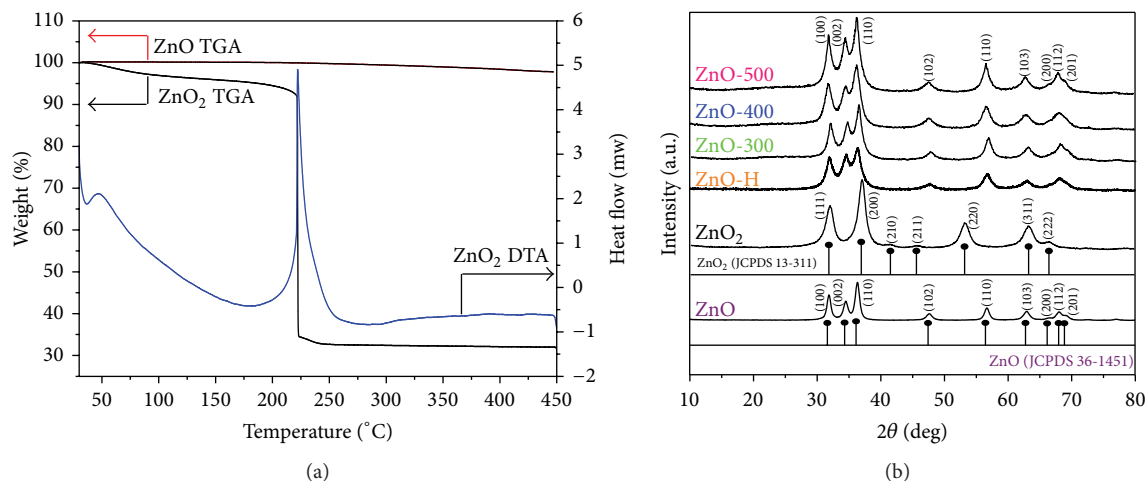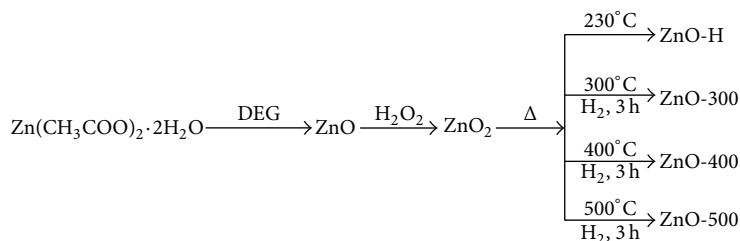
FIGURE 1: (a) TGA (black) and DTA (blue) plot of ZnO_2; (b) XRD of ZnO_2 and different ZnO samples.

SCHEME 1: Flow chart of conversion of ZnO to ZnO_2 and again to different ZnO samples.

3.3. BET Surface Area. Surface area of different samples was determined by NOVA surface area analyzer.

3.4. Scanning Electron Microscopy (SEM). The morphological studies of the prepared ZnO were carried out in field emission scanning electron microscope (FE-SEM SIRION). A drop of well-dispersed particles in water was cast onto a piece of silicon wafer and air-dried. A thin gold coating was applied to avoid charging during scanning and a detailed microscopic study was carried out.

3.5. Electron Paramagnetic Resonance Spectroscopy (EPR). Hydroxyl radicals were detected by EPR-spin trapping technique using spin trapper 5,5-dimethyl-1-pyrroline-N-oxide (DMPO, 0.02 M). Aqueous suspensions of different ZnO samples were drawn separately into quartz capillaries (one end closed) along with DMPO. The capillaries were placed in the EPR tube and spectra were recorded on a Bruker emx X-band EPR spectrometer.

3.6. Photoluminescence (PL) Study. PL spectra were recorded in Jobin Yvon FluoroLog 4 (Horiba) by exciting each equally concentrated ZnO sample solution (aq.) at 370 nm.

3.7. Thermogravimetric Study. Thermogravimetric studies were done in thermogravimetric system (Cahn TG131).

4. Results and Discussion

In order to elucidate proper mechanism of antibacterial activity, ZnO samples with different degrees of physico-chemical properties have been synthesized through a simple route as depicted in Scheme 1. Submicron size ZnO particles were synthesized by polyol method. The as-synthesized ZnO particles were converted to ZnO_2 by reacting with H_2O_2 and heated in presence of H_2 gas at different temperatures.

In this method, various degrees of surface defects (oxygen vacancies) were obtained without much change in particle nature between the samples. The thermogravimetric analysis (TGA) and differential thermal analysis (DTA) of ZnO_2 show a sharp exothermic peak (Figure 1(a)), indicating decomposition of ZnO_2 to ZnO at ~225°C and the reactions were carried out above this temperature.

XRD patterns were obtained for all the samples and are depicted in Figure 1(b). All the reflections were assigned with standard wurtzite structure of ZnO (JCPDS file number 36-1451) while for ZnO_2 the peaks are assigned with pure cubic phase of ZnO_2 (JCPDS file number 13-311). SEM pictures obtained for the samples along with ZnO_2 are shown in Figure 2. It reveals that the pristine ZnO particles are spherical and the size varies between 150 and 250 nm (Figure 2(a)). On treatment with H_2O_2, few smaller sized particles disintegrated (Figure 2(b)) and the larger particles (size 150–250 nm) remain intact even after heating at different temperatures (Figures 2(c), 2(d), 2(e), and 2(f)).
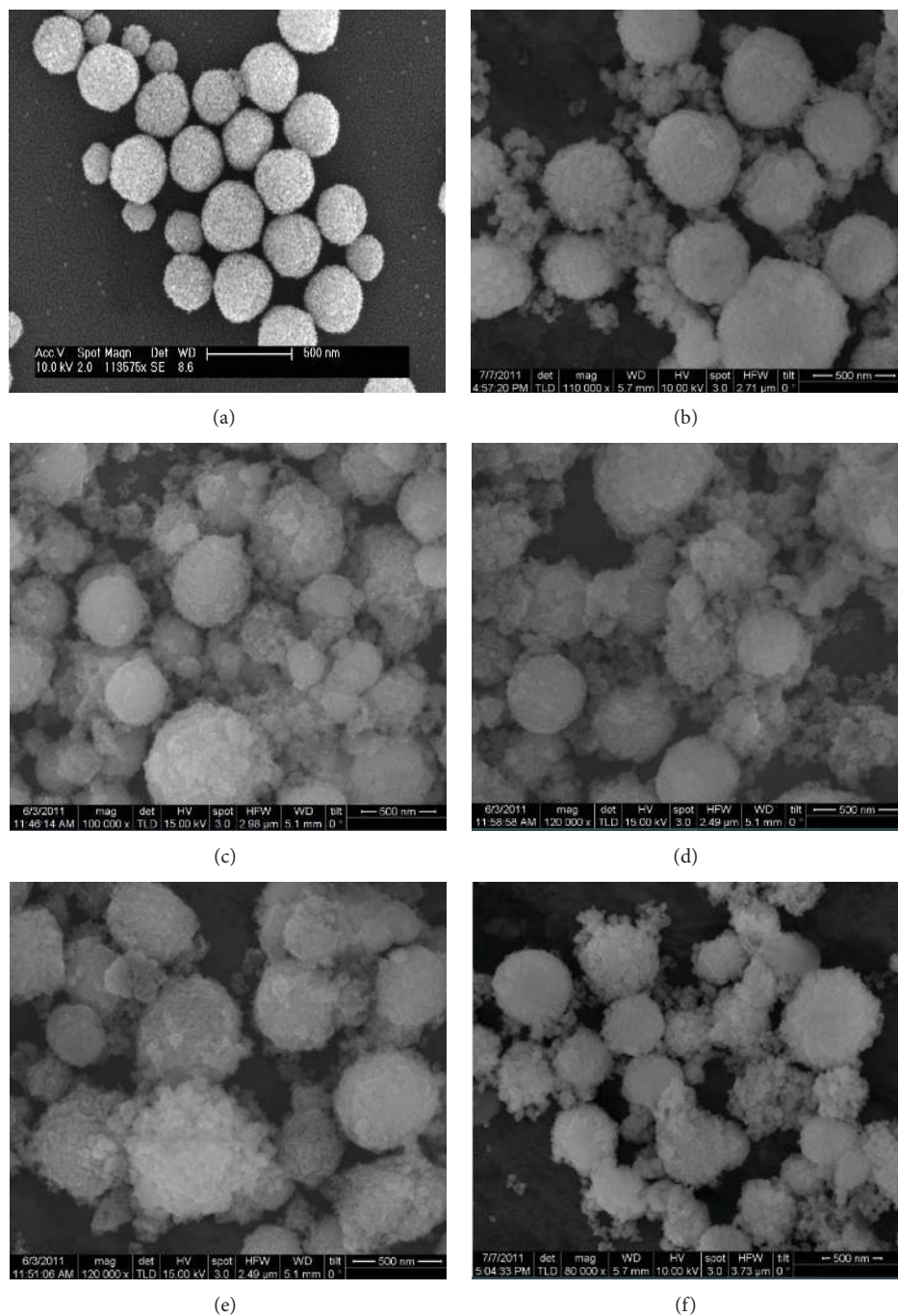
(a)

(b)

(c)

(d)

(e)

(f)

FIGURE 2: SEM micrographs of (a) ZnO, (b) ZnO$_2$, (c) ZnO-H, (d) ZnO-300, (e) ZnO-400, and (f) ZnO-500 (all scale bars: 500 nm).

The physicochemical properties of ZnO samples were tabulated along with MICs as shown in Table 1. To investigate the mechanism of antibacterial activity, MICs were determined with and without treating ZnO samples with GSH.

From pristine ZnO to ZnO-H, the surface area and solubility increase which may be attributed to the smaller fragmentation on treatment with H$_2$O$_2$ and heating, but both solubility and surface area remain unaltered for other samples of ZnO-300 to ZnO-500 (Figure 3(a) and Table 1).

When bactericidal activity was evaluated without GSH treatment, MICs for ZnO to ZnO-500 decrease (Table 1 and Figure 3(b)). The surface area (and hence solubility) of ZnO to ZnO-H increases, but EPR peak-area due to ROS production does not differ much. Bactericidal activity of ZnO NPs increases along with increase in solubility reported earlier [37, 38]. Thus, the decrease in MIC for ZnO to ZnO-H could be accounted by the solubility factor. But the same argument does not fit to account the MIC values of ZnO-300
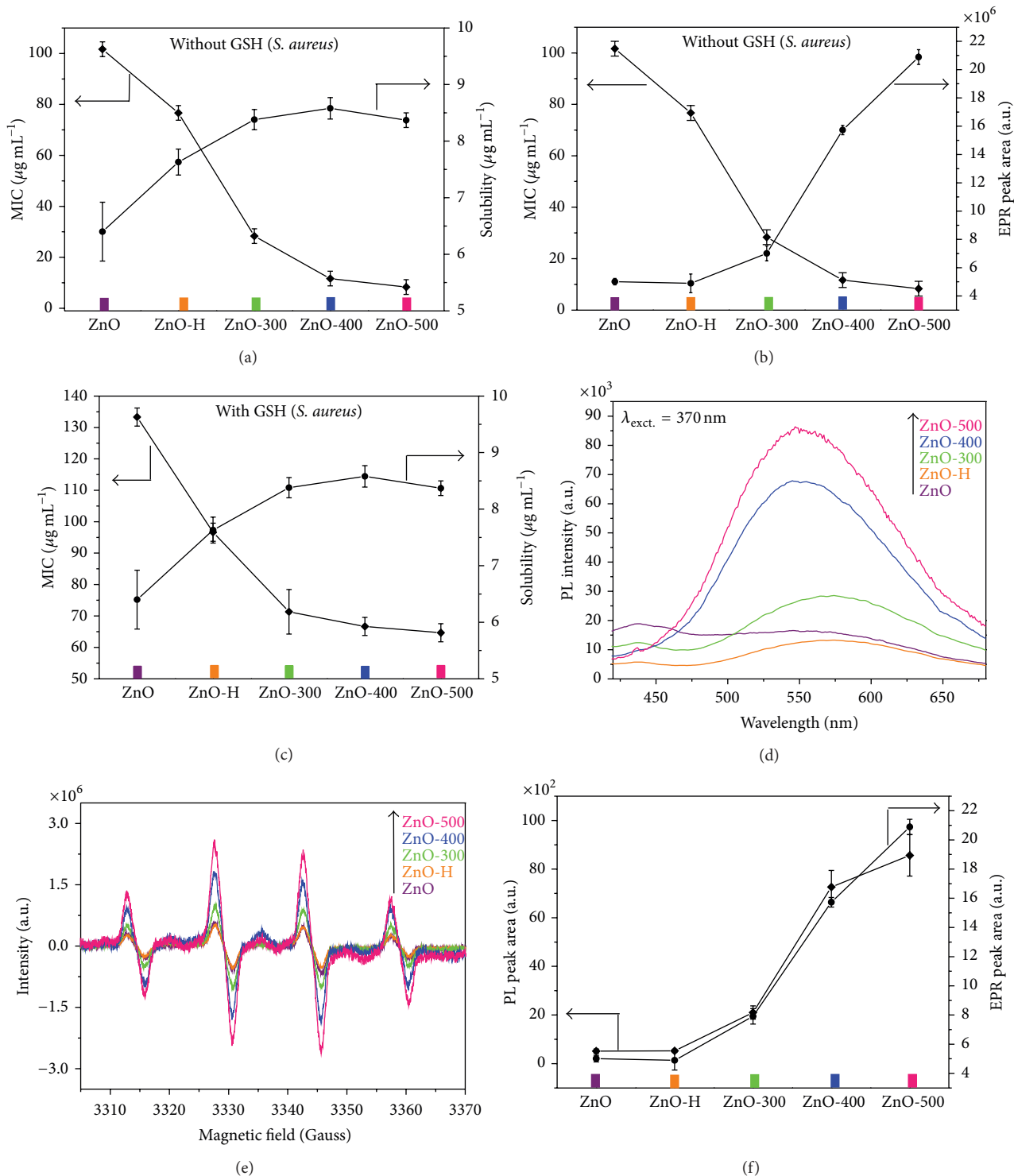
(a)

(b)

(c)

(d)

(e)

(f)

FIGURE 3: Plots of (a) MICs (without GSH) versus solubility, (b) MICs (without GSH) versus EPR peak area, and (c) MICs (with GSH) versus solubility; (d) PL spectra; (e) EPR spectra; and (f) correlation plot of EPR peak area versus PL peak area of different ZnO samples.

to ZnO-500. Solubility (Table 1) of ZnO-300 to ZnO-500 in saline was the same, but MIC value decreases or bactericidal activity increases from ZnO-300 to ZnO-500. So not only the solubility of ZnO samples but also the other factors are responsible for its bactericidal activity.
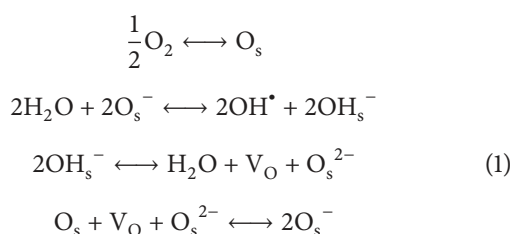
Similarly, when bactericidal activity was determined after GSH (i.e., without ROS production) treatment with ZnO samples, MIC values (Table 1; Figure 3(c)) for ZnO-300 to ZnO-500 were almost the same indicating oxidative stress due to the fact that ROS is the governing factor as other

TABLE 1: Different physicochemical properties and minimum inhibition concentration (MIC) values.

Materials	Surface area (m^2/g)	Solubility ($\mu g\,mL^{-1}$)	EPR peak area (a.u. $\times 10^6$)	S. aureus MIC ($\mu g\,mL^{-1}$)		E. coli MIC ($\mu g\,mL^{-1}$)	
				Without GSH	With GSH	Without GSH	With GSH
ZnO	23.81 ± 0.23	6.40 ± 0.52	05.01 ± 0.23	101.66 ± 2.88	133.33 ± 2.88	125.00 ± 5.00	168.33 ± 2.88
ZnO-H	37.51 ± 0.16	7.63 ± 0.23	04.89 ± 0.66	76.66 ± 2.88	96.66 ± 2.88	96.66 ± 2.88	91.66 ± 2.88
ZnO-300	41.84 ± 0.89	8.38 ± 0.18	07.91 ± 0.53	28.33 ± 2.88	71.33 ± 7.09	43.33 ± 2.88	88.33 ± 2.88
ZnO-400	40.23 ± 0.57	8.58 ± 0.15	15.73 ± 0.33	11.66 ± 2.88	66.66 ± 2.88	26.66 ± 2.88	98.33 ± 2.88
ZnO-500	41.39 ± 0.63	8.37 ± 0.13	20.89 ± 0.52	8.33 ± 2.88	61.66 ± 2.88	13.33 ± 2.88	101.66 ± 2.88

factors like solubility and particle size remain unchanged for ZnO samples. The mechanism by which ROS (i.e., OH$^\bullet$) formed on the ZnO surface is not clear, although some investigations on the nature of the ZnO surface such as chemisorbed OH species after interaction with water produces ROS have been reported [39].

In addition, a little is known about the nature of defect sites on a wet metal oxide surface. The formation of ROS may be explained by assuming the formation of hydroxyl radicals by the reaction of water and (dissolved) oxygen over basic metal oxides [40]:

$$\frac{1}{2}O_2 \longleftrightarrow O_s$$

$$2H_2O + 2O_s^- \longleftrightarrow 2OH^\bullet + 2OH_s^-$$

$$2OH_s^- \longleftrightarrow H_2O + V_O + O_s^{2-} \qquad (1)$$

$$O_s + V_O + O_s^{2-} \longleftrightarrow 2O_s^-$$

The net reaction is $\frac{1}{2}O_2 + H_2O \longleftrightarrow 2OH^\bullet$

where V_O refers to an oxygen vacancy and "s" refers to surface species.

The higher oxygen vacancy, the higher ROS production. This is further shown in the PL spectra of the samples (Figure 3(d)). The green emission between 440 and 700 nm is due to surface oxygen vacancy. The increase in PL peak area (Figure 3(e)) starting from ZnO to ZnO-500 indicates the increase in oxygen vacancy [41]. When such areas are plotted against the corresponding ZnO samples, this shows almost a linear increase and the shape of the curve matches well with the EPR peak area as shown in Figure 3(f). This supports the above proposed mechanism for the ROS production through oxygen vacancy of ZnO.

5. Conclusions

The method adopted for the synthesis of ZnO and ZnO$_2$ is very simple and effective. Different physicochemical properties of ZnO have been varied to validate their influencing nature towards their bactericidal action. When oxidative stress has been nullified by arresting OH$^\bullet$ (hydroxyl) radical with GSH, MICs of ZnO samples (from ZnO to ZnO-H) decrease with the increase of their surface area (particle size

remains the same) and solubility. The effect of oxidative stress towards bactericidal action has been considered (i.e., without GSH treatment) and the MICs of ZnO samples decrease with the increase of the surface defects or ROS production (from ZnO-300 to ZnO-500). Throughout the experiments, particles sizes of ZnO samples were constant and the effect due to physical attack (i.e., direct interactions between the particles and bacteria) is the same and cannot be avoided. Bactericidal properties of ZnO are due to the combination of all depicted mechanisms. It can be concluded that out of all mechanisms oxidative stress developed in bacteria through ROS production of ZnO samples is the most influencing factor for its bactericidal activity.

Conflict of Interests

The authors declare that there is no conflict of interests regarding the publication of this paper.
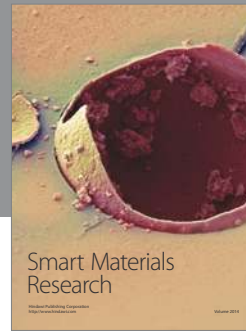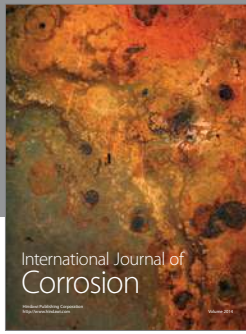
Acknowledgments

References

[1] V. Biju, "Chemical modifications and bioconjugate reactions of nanomaterials for sensing, imaging, drug delivery and therapy," *Chemical Society Reviews*, vol. 43, no. 3, pp. 744–764, 2014.

[2] K. M. L. Taylor-Pashow, J. Della Rocca, R. C. Huxford, and W. Lin, "Hybrid nanomaterials for biomedical applications," *Chemical Communications*, vol. 46, no. 32, pp. 5832–5849, 2010.

[3] S. Ghosh, R. Kaushik, K. Nagalakshmi et al., "Antimicrobial activity of highly stable silver nanoparticles embedded in agar-agar matrix as a thin film," *Carbohydrate Research*, vol. 345, no. 15, pp. 2220–2227, 2010.

[4] S. Ghosh, A. Saraswathi, S. S. Indi, S. L. Hoti, and H. N. Vasan, "Ag@AgI, core@shell structure in agarose matrix as hybrid: synthesis, characterization, and antimicrobial activity," *Langmuir*, vol. 28, no. 22, pp. 8550–8561, 2012.

[5] N. Gao, Y. Chen, and J. Jiang, "Ag@Fe$_2$O$_3$-GO nanocomposites prepared by a phase transfer method with long-term antibacterial property," *ACS Applied Materials and Interfaces*, vol. 5, no. 21, pp. 11307–11314, 2013.

[6] P. Bober, J. Liu, K. S. Mikkonen et al., "Biocomposites of nanofibrillated cellulose, polypyrrole, and silver nanoparticles with electroconductive and antimicrobial properties," *Biomacromolecules*, vol. 15, no. 10, pp. 3655–3663, 2014.

[7] R. Kumar, S. Anandan, K. Hembram, and T. N. Rao, "Efficient ZnO-based visible-light-driven photocatalyst for antibacterial applications," *ACS Applied Materials & Interfaces*, vol. 6, no. 15, pp. 13138–13148, 2014.

[8] S. H. Hwang, J. Song, Y. Jung, O. Y. Kweon, H. Song, and J. Jang, "Electrospun ZnO/TiO$_2$ composite nanofibers as a bactericidal agent," *Chemical Communications*, vol. 47, no. 32, pp. 9164–9166, 2011.

[9] J. Manna, G. Begum, K. P. Kumar, S. Misra, and R. K. Rana, "Enabling antibacterial coating via bioinspired mineralization of nanostructured ZnO on fabrics under mild conditions," *ACS Applied Materials and Interfaces*, vol. 5, no. 10, pp. 4457–4463, 2013.

[10] M. Safarpour, A. Khataee, and V. Vatanpour, "Preparation of a Novel Polyvinylidene Fluoride (PVDF) ultrafiltration membrane modified with reduced graphene oxide/titanium dioxide (TiO$_2$) nanocomposite with enhanced hydrophilicity and antifouling properties," *Industrial & Engineering Chemistry Research*, vol. 53, no. 34, pp. 13370–13382, 2014.

[11] I. Perelshtein, G. Applerot, N. Perkas, J. Grinblat, and A. Gedanken, "A one-step process for the antimicrobial finishing of textiles with crystalline TiO$_2$ nanoparticles," *Chemistry A: European Journal*, vol. 18, no. 15, pp. 4575–4582, 2012.

[12] J. Xiong, Z. Li, J. Chen, S. Zhang, L. Wang, and S. Dou, "Facile synthesis of highly efficient one-dimensional plasmonic photocatalysts through Ag@Cu$_2$O core–shell heteronanowires," *ACS Applied Materials & Interfaces*, vol. 6, no. 18, pp. 15716–15725, 2014.

[13] X. Zhang, T. Zhang, J. Ng, and D. D. Sun, "High-performance multifunctional TiO$_2$ nanowire ultrafiltration membrane with a hierarchical layer structure for water treatment," *Advanced Functional Materials*, vol. 19, no. 23, pp. 3731–3736, 2009.

[14] X. Wang, H.-F. Wu, Q. Kuang, R.-B. Huang, Z.-X. Xie, and L.-S. Zheng, "Shape-dependent antibacterial activities of Ag$_2$O polyhedral particles," *Langmuir*, vol. 26, no. 4, pp. 2774–2778, 2010.

[15] A. Simon-Deckers, S. Loo, M. Mayne-L'Hermite et al., "Size-, composition- and shape-dependent toxicological impact of metal oxide nanoparticles and carbon nanotubes toward bacteria," *Environmental Science and Technology*, vol. 43, no. 21, pp. 8423–8429, 2009.

[16] H. Koga, T. Kitaoka, and H. Wariishi, "In situ synthesis of silver nanoparticles on zinc oxide whiskers incorporated in a paper matrix for antibacterial applications," *Journal of Materials Chemistry*, vol. 19, no. 15, pp. 2135–2140, 2009.

[17] M. Li, S. Pokhrel, X. Jin, L. Mädler, R. Damoiseaux, and E. M. V. Hoek, "Stability, bioavailability, and bacterial toxicity of Zno and iron-doped Zno nanoparticles in aquatic media," *Environmental Science and Technology*, vol. 45, no. 2, pp. 755–761, 2011.

[18] S. Ghosh, V. S. Goudar, K. G. Padmalekha, S. V. Bhat, S. S. Indi, and H. N. Vasan, "ZnO/Ag nanohybrid: synthesis, characterization, synergistic antibacterial activity and its mechanism," *RSC Advances*, vol. 2, no. 3, pp. 930–940, 2012.

[19] Z. Huang, X. Zheng, D. Yan et al., "Toxicological effect of ZnO nanoparticles based on bacteria," *Langmuir*, vol. 24, no. 8, pp. 4140–4144, 2008.

[20] G. Applerot, J. Lellouche, N. Perkas, Y. Nitzan, A. Gedanken, and E. Banin, "ZnO nanoparticle-coated surfaces inhibit bacterial biofilm formation and increase antibiotic susceptibility," *RSC Advances*, vol. 2, no. 6, pp. 2314–2321, 2012.

[21] F. Gladis, A. Eggert, U. Karsten, and R. Schumann, "Prevention of biofilm growth on man-made surfaces: evaluation of antialgal activity of two biocides and photocatalytic nanoparticles," *Biofouling*, vol. 26, no. 1, pp. 89–101, 2010.

[22] B. M. Geilich and T. J. Webster, "Reduced adhesion of Staphylococcus aureus to ZnO/PVC nanocomposites," *International Journal of Nanomedicine*, vol. 8, pp. 1177–1184, 2013.

[23] J. W. Rasmussen, E. Martinez, P. Louka, and D. G. Wingett, "Zinc oxide nanoparticles for selective destruction of tumor cells and potential for drug delivery applications," *Expert Opinion on Drug Delivery*, vol. 7, no. 9, pp. 1063–1077, 2010.

[24] M. J. Osmond and M. J. McCall, "Zinc oxide nanoparticles in modern sunscreens: an analysis of potential exposure and hazard," *Nanotoxicology*, vol. 4, no. 1, pp. 15–41, 2010.

[25] P. T. Sudheesh Kumar, V.-K. Lakshmanan, T. V. Anilkumar et al., "Flexible and microporous chitosan hydrogel/nano ZnO composite bandages for wound dressing: in vitro and in vivo evaluation," *ACS Applied Materials and Interfaces*, vol. 4, no. 5, pp. 2618–2629, 2012.

[26] M. Jensen-Waern, L. Melin, R. Lindberg, A. Johannisson, L. Petersson, and P. Wallgren, "Dietary zinc oxide in weaned pigs—effects on performance, tissue concentrations, morphology, neutrophil functions and faecal microflora," *Research in Veterinary Science*, vol. 64, no. 3, pp. 225–231, 1998.

[27] S. X. Huang, M. McFall, A. C. Cegielski, and R. N. Kirkwood, "Effect of dietary zinc supplementation on *Escherichia coli* septicemia in weaned pigs," *Journal of Swine Health and Production*, vol. 7, no. 3, pp. 109–111, 1999.

[28] R. Brayner, R. Ferrari-Iliou, N. Brivois, S. Djediat, M. F. Benedetti, and F. Fievet, "Toxicological impact studies based on *Escherichia coli* bacteria in ultrafine ZnO nanoparticles colloidal medium," *Nano Letters*, vol. 6, no. 4, pp. 866–870, 2006.

[29] L. Zhang, Y. Jiang, Y. Ding, M. Povey, and D. York, "Investigation into the antibacterial behaviour of suspensions of ZnO nanoparticles (ZnO nanofluids)," *Journal of Nanoparticle Research*, vol. 9, no. 3, pp. 479–489, 2007.

[30] X. Li, Y. Xing, Y. Jiang, Y. Ding, and W. Li, "Antimicrobial activities of ZnO powder-coated PVC film to inactivate food pathogens," *International Journal of Food Science and Technology*, vol. 44, no. 11, pp. 2161–2168, 2009.

[31] C. Karunakaran, V. Rajeswari, and P. Gomathisankar, "Antibacterial and photocatalytic activities of sonochemically prepared ZnO and Ag-ZnO," *Journal of Alloys and Compounds*, vol. 508, no. 2, pp. 587–591, 2010.

[32] N. Jones, B. Ray, K. T. Ranjit, and A. C. Manna, "Antibacterial activity of ZnO nanoparticle suspensions on a broad spectrum of microorganisms," *FEMS Microbiology Letters*, vol. 279, no. 1, pp. 71–76, 2008.

[33] I. Sondi and B. Salopek-Sondi, "Silver nanoparticles as antimicrobial agent: a case study on *E. coli* as a model for Gram-negative bacteria," *Journal of Colloid and Interface Science*, vol. 275, no. 1, pp. 177–182, 2004.

[34] G. Appierot, A. Lipovsky, R. Dror et al., "Enhanced antibacterial activity of nanocrystalline ZnO due to increased ROS-mediated cell injury," *Advanced Functional Materials*, vol. 19, no. 6, pp. 842–852, 2009.

[35] A. Lipovsky, Z. Tzitrinovich, H. Friedmann, G. Applerot, A. Gedanken, and R. Lubart, "EPR study of visible light-induced

ros generation by nanoparticles of ZnO," *Journal of Physical Chemistry C*, vol. 113, no. 36, pp. 15997–16001, 2009.

[36] L. K. Adams, D. Y. Lyon, and P. J. J. Alvarez, "Comparative ecotoxicity of nanoscale TiO$_2$, SiO$_2$, and ZnO water suspensions," *Water Research*, vol. 40, no. 19, pp. 3527–3532, 2006.

[37] W. Bai, Z. Zhang, W. Tian et al., "Toxicity of zinc oxide nanoparticles to zebrafish embryo: a physicochemical study of toxicity mechanism," *Journal of Nanoparticle Research*, vol. 12, no. 5, pp. 1645–1654, 2010.

[38] M. Li, L. Zhu, and D. Lin, "Toxicity of ZnO nanoparticles to *Escherichia coli*: mechanism and the influence of medium components," *Environmental Science & Technology*, vol. 45, no. 5, pp. 1977–1983, 2011.

[39] G. Sengupta, H. S. Ahluwalia, S. Banerjee, and S. P. Sen, "Chemisorption of water vapor on zinc oxide," *Journal of Colloid And Interface Science*, vol. 69, no. 2, pp. 217–224, 1979.

[40] K. B. Hewett, L. C. Anderson, M. P. Rosynek, and J. H. Lunsford, "Formation of hydroxyl radicals from the reaction of water and oxygen over basic metal oxides," *Journal of the American Chemical Society*, vol. 118, no. 29, pp. 6992–6997, 1996.

[41] K. Vanheusden, C. H. Seager, W. L. Warren, D. R. Tallant, and J. A. Voigt, "Correlation between photoluminescence and oxygen vacancies in ZnO phosphors," *Applied Physics Letters*, vol. 68, no. 3, pp. 403–405, 1996.

Journal of
Nanotechnology

International Journal of
Corrosion

International Journal of
Polymer Science

Smart Materials
Research

Journal of
Composites

BioMed
Research International

Journal of
Metallurgy

Journal of
Materials

Hindawi

Submit your manuscripts at
http://www.hindawi.com

Journal of
Nanoparticles

Advances in
Materials Science and Engineering

Scientifica

Journal of
Nanomaterials

The Scientific
World Journal

International Journal of
Biomaterials

Journal of
Nanoscience

Journal of
Coatings

Journal of
Crystallography

Journal of
Ceramics

Journal of
Textiles